

A Review of the Mechanics of Dragline Spider Silk

Leo Sandstrom

International French School, Singapore

ABSTRACT

Spider silks demonstrate extraordinary mechanical performance. They rely on an intricate hierarchical structure that gives rise to unique properties. Of the many types of spider silks that are produced, dragline spider silk has attracted the most research attention due its extremely high strength. Since data on dragline spider silk is readily available, much can be understood about the nature of spider silk by analyzing the structure of dragline spider silk. Moreover, the study of spider silk can inspire the design of new materials. Here, we review the structure of dragline silk, present a particular material model to explain their behavior, and discuss the potential outlook in the area.

Introduction

Biological materials often demonstrate extraordinary mechanical properties and are a source of inspiration for material development. An example of such a material is spider silk, which is composed of protein-based biopolymer filaments or threads. Spider silk is strong, elastic, highly stretchable, and tough. Such outstanding mechanical properties make it suitable for a wide range of activities a spider undergoes, such as wrapping of eggs and capturing insects. Moreover, spider silk's unique structure as well as its high strength to weight ratio has prompted researchers to look into the mechanisms that govern its mechanical properties (Work, 1978; Gosline, et al., 1986) . While spiders produce many different types of silk, much of the research has focused on dragline silk, which is the backbone of the spider's web. Dragline silk is also the strongest type of silk produced by spiders, and rivals the strength of many synthetic materials. For instance, the strength of spider silk was measured to be 1.1 GPa (Griffiths and Salanitri, 1980) which is comparable to the strength of stainless steel and Nylon. However, the density of spider silk is roughly six times less than that of stainless steel, making it an extremely strong material relative to its weight. Fibers made of dragline spider silk are also comparable to some of the strongest synthetic fibers. Work (Work, 1976) has tested the strength of dragline spider silk fibers and has found a strength of around 1.8 GPa. Indeed, its specific strength, defined as the strength divided by the density of a material, is comparable to glass fiber. Not all dragline silk possess the same properties. Variations in mechanical properties can be present in different species of spider and across spiders of the same species with differing diets. Here, we review the structure of dragline silk, present a particular material model to explain their behavior, and discuss the potential outlook in the area. It is hoped that this review can reinforce the applicability of dragline silk in industrial use.

Structure of Spider Silk

The morphology of dragline spider silk has been extensively studied across a wide range of length scales. Much of the understanding of the behavior of spider silk is derived from atomistic simulations of its structure (Meyers, et al., 2013). Scanning electron microscope images taken on a strand of dragline silk (Riekel, et al., 2001) demonstrate that the fibers are a composite of two fibers of different sizes: major ampullate silk fibers, with diameters on the order of a few microns, and minor ampullate fibers which are typically half the diameter size

of the former. Transmission electron images (Rousseau, et al., 2007) taken on single fiber reveals the underlying nanoscale structure of the fibers, consisting of fibrils that are aligned parallel to the axis of the fiber. Atomic force microscopy (Gould, et al., 1999) images on an even smaller scale demonstrate the presence of β -sheet nanocrystalline domains that surround the amorphous regions. Both the amorphous and crystalline domains are major components that give rise to the mechanical behavior of spider silk. In particular, the crystalline regions endow the spider silk with its high strength, while the amorphous regions provide elasticity. On a molecular level, the β -sheets hold the molecules together and provide stiffness, while the amorphous regions allow molecular mobility (Gosline, et al., 1986). A typical stress-strain curve of spider silk exhibits several unique regions each of which correspond to a different nanostructural behavior (Fig 1). At low stresses, the hydrogen bonds between amorphous chains give rise to a high modulus, and the behavior is elastic. At this elastic regime, the amorphous chains are being stretched. Beyond this range, the hydrogen bonds are broken, and the stiffness of the spider silk is given by the entropic unfolding of the protein domains. The spider silk then exhibits major stiffening due to the presence of the β -sheet nanocrystalline domains, after which the silk exhibits a stick slip behavior before failure.

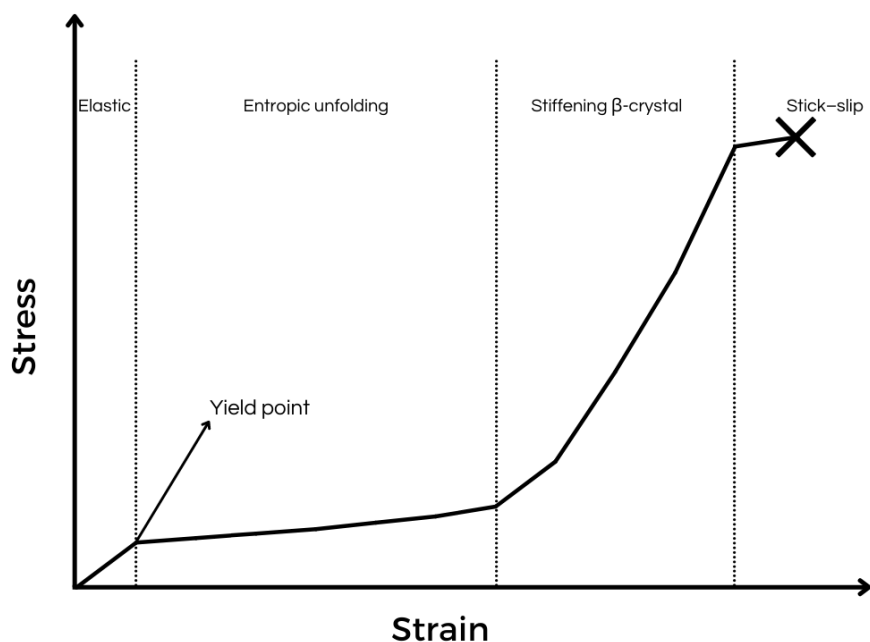


Figure 1. Stress-strain behavior of spider silk. At low stresses, amorphous chains are being stretched. Beyond this range, the hydrogen bonds are broken, and the stiffness of the spider silk is given by the entropic unfolding of the protein domains. The spider silk then exhibits major stiffening due to the presence of the β -sheet nanocrystalline domains. Prior to fracture, the silk exhibits a stick slip behavior.

Spider Silk Elasticity

As mentioned earlier, spider silk is inherently semicrystalline—consisting of amorphous chains that are surrounded by rigid crystals. In the absence of water, the amorphous chains are also connected by hydrogen bonds. However, when water is present in the amorphous regions, the hydrogen bonds do not form (Fig 2), and thus the amorphous phase becomes less stiff.

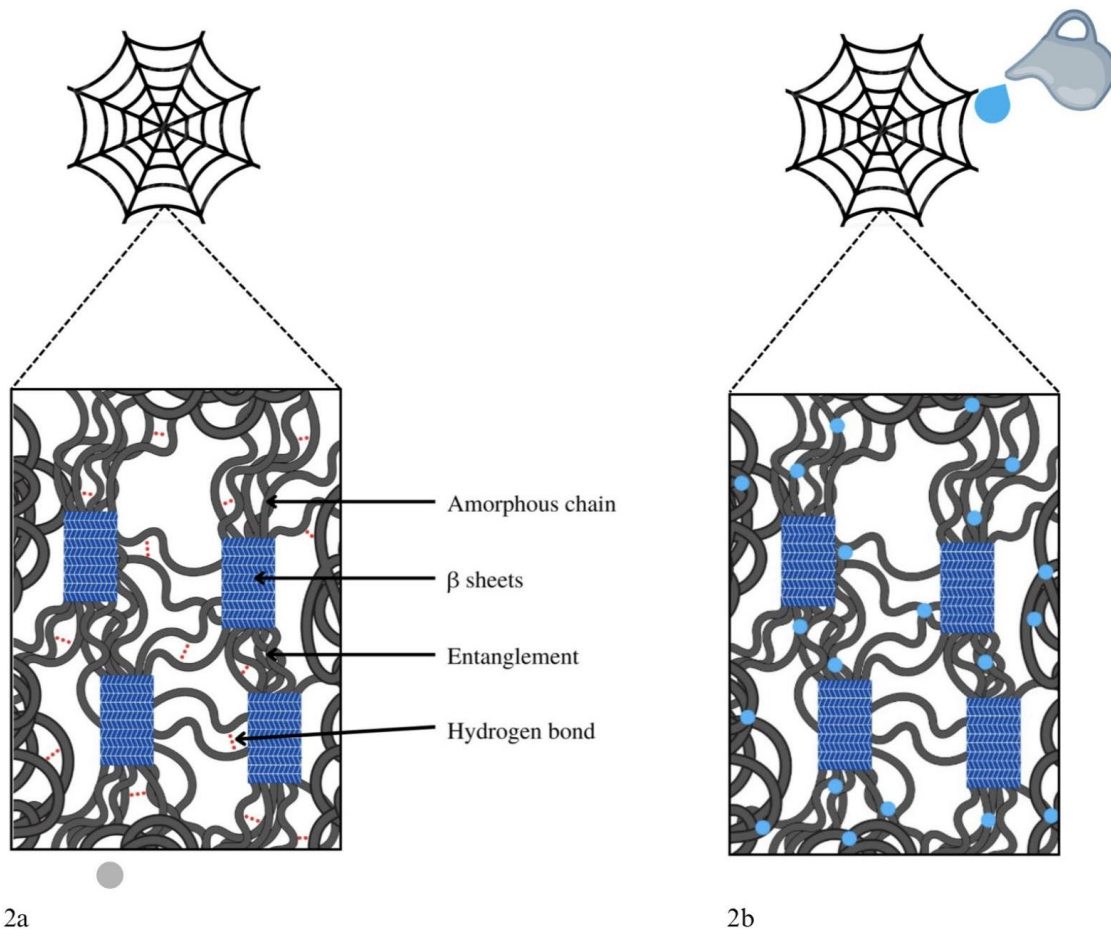


Figure 2. Dragline silk structure in the dry and wet state. As seen in figure 2a, amorphous chains are surrounded by β sheets, which act like rigid crystals. As well as being entangled, these dry amorphous chains are further linked by hydrogen bonds. As seen in figure 2b, when the silk is wet, hydrogen bonds do not form, making the amorphous phase less stiff.

In the absence of hydrogen bonds, the chains in the amorphous regions form a random-coil orientation. Termonia formulated a theoretical model of spider silk elasticity based on this picture. We now highlight the theoretical model of Termonia and discuss its implications. The model assumes that when stress is applied to the network, the hydrogen bonds between the amorphous regions break at a certain rate that depends on the local stress. Parameters of the bond breaking rate can be estimated based on the yield point of the spider silk network. Unlike the amorphous chains, the crystalline regions are assumed to remain intact, because their stiffness is extremely high. After a hydrogen bond in the amorphous region is broken, the load is transferred to the amorphous chain strand. The stress in an amorphous chain is given by:

$$\sigma = E_a \sqrt{\langle n_e \rangle} f(\lambda_i, n_e) \quad (1)$$

where E_a is the modulus of the amorphous chain and n_e is the number of monomers between entanglements. The stiffness of an amorphous polymer chain is given by

$$E_a = 3NkT$$

(2)

where N is the number of polymers in a chain, K is the boltzmann constant and T is the temperature. Note that the stiffness is calculated based on rubber elasticity theory and thus assumes that the region is entirely amorphous. However, some regions have crystal β -sheets surrounding them. For these chains, the modulus is given by:

$$E_{a\beta} = 6E_a$$

(3)

The chains near the β -sheets are indeed stiffer because chains exiting the β -sheet are confined. When simulations are conducted on the wet dragline silk, the stress-strain curve exhibits a linear behavior up to a stretch of about 2. After a stretch of two, the material strain stiffens, until the amorphous chains reach their extension limit and break. After the amorphous chains sequentially break, the network fails. When simulations are conducted on a dry network, only the initial portion of the stress stretch curve is linear. Deviations from linearity begin to happen at a stretch of about 1.02, which is due to the breakage of hydrogen bonds in the amorphous regions. Note that once the hydrogen bonds are broken, the behavior of the dry dragline silk must be the same as the wet dragline silk since the only difference between the two networks would be the presence of hydrogen bonds in the former. As expected, the simulations demonstrate that beyond a stretch of 1.1, the two curves overlap. Next, the effect of crystallinity on mechanical behavior was studied. When the modulus of all amorphous chains is assumed to be uniform, that is, the material does not have any crystalline regions, the strength drops by about 5 times. The modulus is also drastically reduced. This demonstrates the importance of the crystalline regions in giving dragline spider silk its exceptional properties. The effect of crystalline size was also studied, where it was shown that the strength of the spider silk decreases when larger crystals are used. The authors attribute this effect to the increased volume fraction of the thin, high modulus layer. The model of spider silk elasticity gives us great insight to applications of spider silk, which we will discuss in the next section.

Applications and Future Outlook

The production of spider silk can be useful for many biological applications. For instance, combining fiber twisting and braiding of silk fibers has been used as means of artificial ligament replacement (Altman, et al., 2002). Spider silk-based films have also been synthesized and find promising applications in wound dressings (Hümmerich, et al., 2006). Research into spider-silk based hydrogels has also been promising. The hydrogels are formed by self-assembled nanofibers of silk that transform into a hydrogel fiber network over time (Ramensee, et al., 2006). This provides a vast area of biological applications since hydrogels for tissue engineering (Hassan and Peppas, 2006), drug delivery (Langer, 1998), and soft machines (Calvert, 2009). Spider silk-based fibers also find promising applications in composite structures. As mentioned earlier, spider silk is strong, tough, and light-weight, making them ideal for fiber composite synthesis (Arcidiacono, et al., 2006). Given the recent popularity of soft composites, the authors believe that silk-derived soft composites is an extremely promising area of research. Although spider silk exhibits excellent mechanical properties and its mechanics are relatively well studied, a major bottleneck in the applications of spider silk appears to be its production. In particular, the inability to express a complete strand of spider silk proteins, from which spider silk fibers can be synthesized, is a major limitation at the genetic level. An issue lies in maintaining the adequate quality of spider to silk which necessitates the full recapitulation of the silk properties. Every protein domain must be present and accurately recreated due to all these domains being key to the quality of the silk. However, once the expression of a full length spider silk is achieved, silk can be recreated at the low costs needed to encourage its commercialisation in a vast variety of industries.

Acknowledgments

I would like to thank my advisor for the valuable insight provided to me on this topic.

References

1. Work, R. W. (1978). Mechanism for the deceleration and support of spiders on draglines. *Transactions of the American Microscopical Society*, 180-191.
2. Gosline, J. M., DeMont, M. E., & Denny, M. W. (1986). The structure and properties of spider silk. *Endeavour*, 10(1), 37-43.
3. Griffiths, J. R., & Salanitri, V. R. (1980). The strength of spider silk. *Journal of Materials Science*, 15, 491-496.
4. Work, R. W. (1976). The force-elongation behavior of web fibers and silks forcibly obtained from orb-web-spinning spiders. *Textile Research Journal*, 46(7), 485-492.
5. Meyers, M. A., McKittrick, J., & Chen, P. Y. (2013). Structural biological materials: critical mechanics-materials connections. *science*, 339(6121), 773-779.
6. Riekel, C., Craig, C. L., Burghammer, M., & Müller, M. (2001). Microstructural homogeneity of support silk spun by *Eriophora fuliginea* (CL Koch) determined by scanning X-ray microdiffraction. *Naturwissenschaften*, 88, 67-72.
7. Rousseau, M. E., Hernández Cruz, D., West, M. M., Hitchcock, A. P., & Pézolet, M. (2007). *Nephila clavipes* spider dragline silk microstructure studied by scanning transmission X-ray microscopy. *Journal of the American Chemical Society*, 129(13), 3897-3905.
8. Gould, S. A. C., Tran, K. T., Spagna, J. C., Moore, A. M. F., & Shulman, J. B. (1999). Short and long range order of the morphology of silk from *Latrodectus hesperus* (Black Widow) as characterized by atomic force microscopy. *International journal of biological macromolecules*, 24(2-3), 151-157.
9. Gosline, J. M., DeMont, M. E., & Denny, M. W. (1986). The structure and properties of spider silk. *Endeavour*, 10(1), 37-43.
10. Altman, G. H., Horan, R. L., Lu, H. H., Moreau, J., Martin, I., Richmond, J. C., & Kaplan, D. L. (2002). Silk matrix for tissue engineered anterior cruciate ligaments. *Biomaterials*, 23(20), 4131-4141.
11. Hümmerich, D., Slotta, U., & Scheibel, T. (2006). Processing and modification of films made from recombinant spider silk proteins. *Applied Physics A*, 82, 219-222.

12. Rammensee, S., Hümmerich, D., Hermanson, K. D., Scheibel, T., & Bausch, A. R. (2006). Rheological characterization of hydrogels formed by recombinantly produced spider silk. *Applied Physics A*, 82, 261-264.
13. Hassan, C. M., & Peppas, N. A. (2000). Structure and applications of poly (vinyl alcohol) hydrogels produced by conventional crosslinking or by freezing/thawing methods. *Biopolymers· PVA hydrogels, anionic polymerisation nanocomposites*, 37-65.
14. Langer, R. (1998). Drug delivery and targeting. *Nature*, 392(6679 Suppl), 5-10.
15. Calvert, P. (2009). Hydrogels for soft machines. *Advanced materials*, 21(7), 743-756.
16. Arcidiacono, S., Mello, C. M., Butler, M., Welsh, E., Soares, J. W., Allen, A., ... & Chase, S. (2002). Aqueous processing and fiber spinning of recombinant spider silks. *Macromolecules*, 35(4), 1262-1266.